Dalton Transactions

PAPER

View Article Online
View Journal | View Issue

Cite this: *Dalton Trans.*, 2016, **45**, 4791

Magnetofluorescent micelles incorporating Dy^{III}–DOTA as potential bimodal agents for optical and high field magnetic resonance imaging†

Michael Harris,[a] Luce Vander Elst,[b,c] Sophie Laurent[b,c] and Tatjana N. Parac-Vogt*[a]

Received 8th December 2015,
Accepted 18th January 2016

DOI: 10.1039/c5dt04801j

www.rsc.org/dalton

Dysprosium(III) was coordinated to four 1,4,7,10-tetraazacyclododecane-1,4,7,10-tetraacetic acid (DOTA) bisamide derivatives functionalized with amphiphilic *p*-dodecylaniline and *p*-tetradecylaniline in a differing *cis*- and *trans*-orientation. The complexes were assembled into mono-disperse micelles having size distribution maxima ranging from 10 to 15 nm and the magnetic and optical properties of the micelles were examined in detail. The micelles show characteristic Dy(III) emission with quantum yields reaching 0.8%. The transverse relaxivity r_2 per Dy(III) ion at 500 MHz and 310 K reaches maximum values of *ca.* 20 s^{-1} mM^{-1} which is a large increase when compared to a value of 0.8 s^{-1} mM^{-1} observed for Dy^{III}–DTPA. The micelles were stable in water when incubated at 37 °C for 1 week and showed no relaxivity decrease when measured in the presence of 4% (w/v) human serum albumin. The efficient T_2 relaxation, especially at strong magnetic fields, is sustained by the high magnetic moment of the dysprosium(III) ion, the coordination of water molecules and long rotational correlation times.

Introduction

Magnetic resonance imaging (MRI), positron emission tomography (PET), fluorescence imaging and bioluminescence are powerful *in vivo* techniques used in clinical diagnostics. Contrast agent bimodality is seen as an approach to overcome the inherent limitations that are associated with one individual technique. MRI is ideal for whole body images due to its good spatial resolution but suffers from low sensitivity, requiring high concentrations of Gd(III)-based contrast agents (CAs).[1] Complimentary to this, luminescence-based imaging can provide high-resolution images, but this technique is only suitable for thin tissue samples because of the low optical transparency of biological tissue.[2]

CAs currently used in MRI are based on complexes of gadolinium(III) with diethylenetriaminepentaacetic acid (DTPA) or 1,4,7,10-tetraazacyclododecane-1,4,7,10-tetraacetic acid (DOTA), which cause shortening of the longitudinal relaxation time (T_1) of water protons resulting in a positive contrast, but suffer from dramatic loss of efficiency at high magnetic fields.[1]

Alternatively, iron oxide nanoparticles can be used to accelerate the transverse relaxation time of water protons (T_2) resulting in a negative contrast[3–7] and for enhancing functional MRI studies into brain activity.[8] Decreasing the molecular tumbling rate by conjugation of chelates to polymers or dendrimers,[9–13] non-covalent interaction with human serum albumin[14–17] or by incorporation into supramolecular micelles or liposomes[18–20] has been investigated to increase the CA's relaxation performance.

Recent efforts to enhance imaging performance of CAs combine magnetic and luminescent properties with the aim to achieve a good resolution with high sensitivity thereby allowing visualisation of samples in exquisite detail.[21–24] DTPA and DOTA have been investigated attached to several organic dyes[25,26] and transition metal complexes[27–30] where their bimodal applications have been exploited. The design and characterization of non-fluorescent micelles,[31] fluorescent liposomes,[32,33] and nanoparticles enhancing the longitudinal[34] or transverse relaxation time[35–38] have also been reported. The use of lanthanide systems circumvents restrictions of bio-conjugates such as short luminescence lifetimes, small Stokes' shifts, and photobleaching. Dysprosium(III) ions possess a very high magnetic moment (μ = 10.6μ_B) and an asymmetric ground state, therefore it displays an efficient transverse relaxivity at strong magnetic fields, which makes it suitable for designing negative (T_2) contrast agents.[39–42]

[a]*KU Leuven, Department of Chemistry, Celestijnenlaan 200F, 3001 Leuven, Belgium. E-mail: tatjana.vogt@chem.kuleuven.be*
[b]*Department of General, Organic and Biomedical Chemistry, NMR and Molecular Imaging Laboratory, University of Mons, 7000 Mons, Belgium. E-mail: luce.vanderelst@umons.be*
[c]*CMMI - Center for Microscopy and Molecular Imaging, 6041 Gosselies, Belgium*

†Electronic supplementary information (ESI) available. See DOI: 10.1039/c5dt04801j

Additionally, sensitized Dy(III) ions can emit blue light of approx. 480 nm and yellow light of approx. 575 nm.[43,44] Therefore, magnetic and optical properties of Dy(III) chelates make them interesting candidates for use in bimodal imaging applications.

Recently we reported on amphiphilic DTPA-bisamides based Dy(III) and Tb(III) complexes which showed favourable magnetic and optical properties with very high transverse relaxivities.[45,46] In this paper we developed amphiphilic macrocyclic DOTA chelators which are expected to form stronger complexes[1] with lanthanides, and in addition, the reduced occupied space around the Dy(III) ion in comparison to DTPA could provide better relaxation characteristics by allowing enhanced water exchange kinetics. The DOTA ligands have been shown to form stable complexes with Tb(III), representing the first example of Tb(III) compounds that had been characterized for bimodal application, showing promising optical and magnetic properties.[47] Since Dy(III) has a higher magnetic moment than Tb(III), in this paper we explore the general applicability of this approach by examining the Dy(III)–DOTA based complexes as potential MRI contrast agents. Furthermore, the ligands were derivatized with *p*-alkyl phenyl amides which can serve as "antennae" for energy transfer to Dy(III), resulting in observable luminescence. The amphiphilic complexes were assembled into micellar aggregates, and the relaxation, luminescence efficiency and stability of the resulting nano-aggregates has been investigated in detail.

Results and discussion

Synthesis of ligands, complexes and micelles

Four DOTA bisamide derivatives with long hydrophobic side chains were synthesized by analogous procedure reported earlier by our group, starting from cyclen to produce compounds with a *cis*- or *trans*-orientation. For the *cis*-orientation (Scheme 1), cyclen is reacted with 2 equivalents of *tert*-butyl bromoacetate according to a modified reported procedure which leaves two available amines.[48] *trans*-Orientation is achievable by modifying another reported procedure (Scheme 2),[49] by protecting two amines of the cyclen ring with benzyl chloroformate, then reacting the other two available amines with *tert*-butyl bromoacetate. After selective deprotection by hydrogenation, two free amines are available in a *trans*-orientation. After conversion of *p*-dodecyl aniline and *p*-tetradecyl aniline to chloro acetamides with chloro acetylchloride, combination with the free amines of the *cis*- or *trans*-DOTA and deprotection of the acids results in the final DOTA-bisamides. All ligands have been characterised by nuclear magnetic resonance spectroscopy, mass spectrometry, and IR spectroscopy.

The four ligands were coordinated to dysprosium(III) in pyridine according to a known procedure.[50] The absence of free lanthanide ions has been verified by the addition of an arsenazo indicator solution.[51] The complex formation has been established by mass spectrometry (E.S.I) and IR spectroscopy.

The lanthanide complexes of *cis*-DOTA-bis-*p*-dodecylphenyl amide, *cis*-DOTA-bis-*p*-tetradecylphenyl amide, *trans*-DOTA-bis-*p*-dodecylphenyl amide and *trans*-DOTA-bis-*p*-tetradecylphenyl amide consist of a hydrophilic centre and two hydrophobic tails with a phenyl and a chain of 12 or 14 carbon atoms. The amphiphilic nature permits them to be incorporated into mixed micelles, creating slowly tumbling supramolecular structures and limiting local motions of the lanthanide complexes. Micelles were formed by mixing one equivalent of the dysprosium complex with twelve equivalents of phospholipid (DPPC) and 6.5 equivalents of surfactant (Tween 80®). Photon correlation spectroscopy measurements showed mono-disperse size distribution profiles (E.S.I). This procedure resulted in completely transparent micelle solutions with particle size distribution maxima ranging from 10–15 nm.

Photophysical properties

Due to the $\pi \rightarrow \pi^*$ transitions of the ligands, all dysprosium micelles display well defined absorption bands (Fig. 1). The Dy-*cis*-DOTA-BC_{12}PheA, Dy-*cis*-DOTA-BC_{14}PheA, Dy-*trans*-DOTA-BC_{12}PheA, and Dy-*trans*-DOTA-BC_{14}PheA assembled with phospholipid DPPC and surfactant Tween 80® form micelles that are characterized with a ligand centred band in the range 220–300 nm with a maximum at around 240 nm in the absorption spectrum, corresponding to the ligand electronic transitions. It was observed that the different alkyl chain lengths and orientations show slightly shifted spectrum maxima which are most likely caused by the varying aggregation of the ligand into the phospholipid micelles. The excitation spectra (Fig. 2) shows that ~265 nm is the most efficient

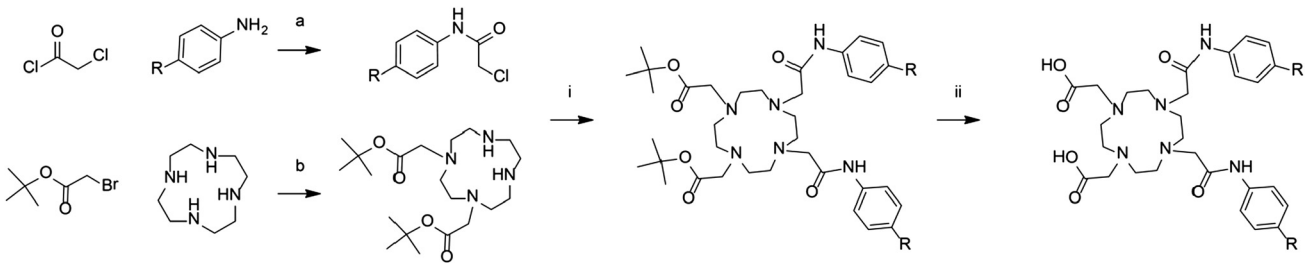

Scheme 1 Synthesis of *cis*-DOTA-BC_nPheA. (a) Dichloromethane, potassium carbonate (2.5 eq.), room temp 30 min, reflux 4 hours. (b) Chloroform, DIPEA (2,5 eq.), 12 hours. (i) Acetonitrile, potassium carbonate (3 eq.), reflux 12 hours. (ii) TFA/dichloromethane, room temp 12 hours.

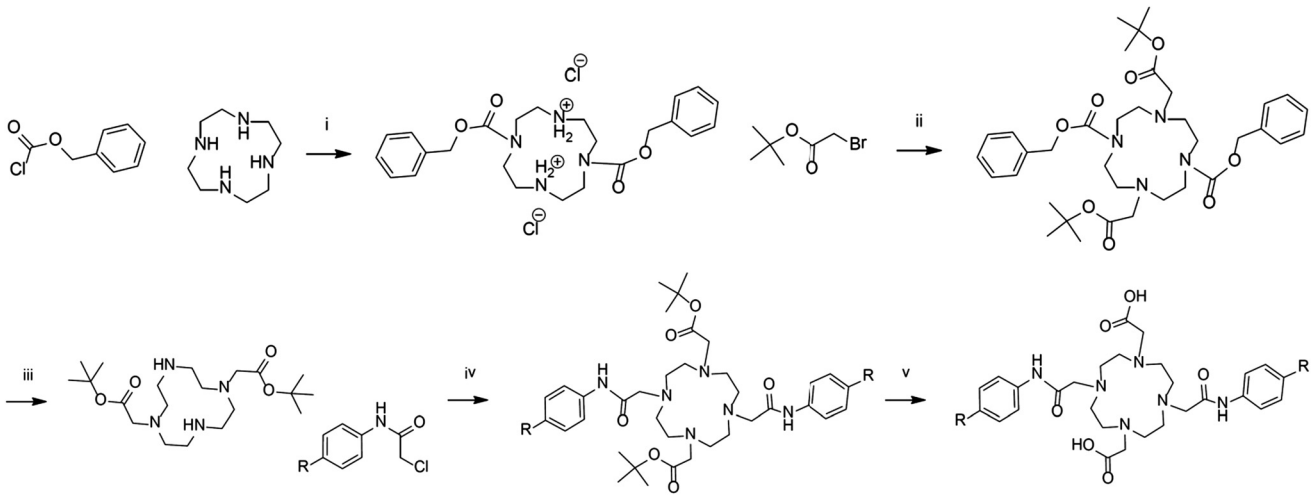

Scheme 2 Synthesis of *trans*-DOTA. (i) Chloroform, 0 °C, 24 hours. (ii) Acetonitrile, DIPEA (5 eq.), 60 °C, 12 hours. (iii) Methanol, H_2 (40 p.s.i), Pd–C catalyst (5% Pd, 20 wt%), 12 hours. (iv) Acetonitrile, potassium carbonate (3 eq.), reflux 12 hours. (v) TFA/dichloromethane, room temp. 12 hours. R = alkyl *n*-$C_{12}H_{25}$ and *n*-$C_{14}H_{29}$.

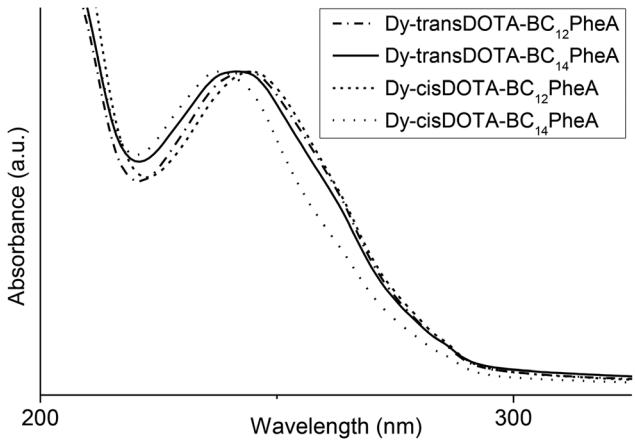

Fig. 1 Normalized absorbance spectrum of Dy(III) micelles in water (pH 7.4, 0.1 wt%, 298 K).

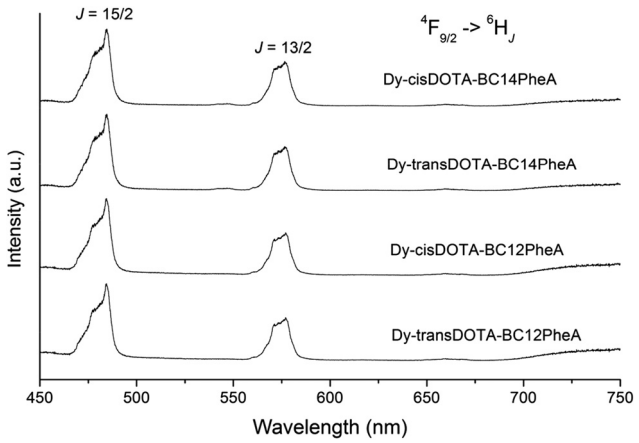

Fig. 3 Corrected and normalized luminescence spectrum of Dy(III) micelles in water (λ_{exc} 265 nm, pH 7.4, 0.1 wt%, 298 K).

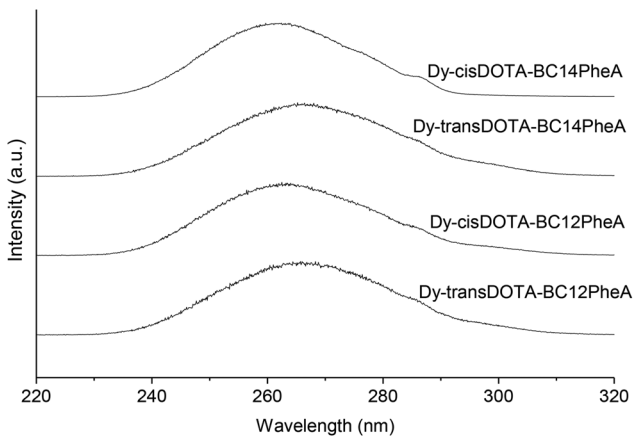

Fig. 2 Corrected and normalized excitation spectrum of Dy(III) micelles in water (λ_{emi} 578 nm, pH 7.4, 0.1 wt%, 298 K).

wavelength for the Dy(III) ion with a small shift between the *cis*- and *trans*-orientation.

The emission spectra of the micelles display sharp emission bands attributed to the $^4F_{9/2} \rightarrow {}^6H_J$ (J = 15/2–9/2) transition of the Dy(III) ion upon excitation at 265 nm (Fig. 3). The efficient energy transfer from ligand to Dy(III) is maintained since little ligand-centred emission is detected. The NIR emission of the dysprosium micelles has also been measured, but very low signal intensity has been observed. In general, it is very difficult to observe Dy(III) NIR luminescence in aqueous solution due to quenching of the excited states through vibronic coupling with water hydroxyl group vibrations.[52]

Luminescence lifetimes in both H_2O and D_2O solutions have been obtained after a mono-exponential fit of the luminescence decays, which indicates the presence of only one type of luminescent lanthanide species in the micellar structures. Luminescence lifetimes in H_2O equal 14.9, 17.5, 11.1 and

10.1 μs for micelles consisting of Dy-*cis*-DOTA-BC_{12}PheA, Dy-*cis*-DOTA-BC_{14}PheA, Dy-*trans*-DOTA-BC_{12}PheA, and Dy-*trans*-DOTA-BC_{14}PheA respectively. In D_2O, luminescence lifetimes up to 39.5, 41.4, 33.95, and 32.6 μs are obtained for the same series respectively. Within the uncertainty of the luminescence method, the following phenomenological eqn (1) for Dy(III)-polyaminocarboxylate systems[53,54] has been employed to determine the number of coordinated water molecules q with an accuracy of ±0.2–0.3:

$$q_{Dy}(H_2O) = 21.1k_{obs} - 0.60 \quad (1)$$

in which $\Delta k_{obs} = 1/\tau_{H_2O} - 1/\tau_{D_2O}$ is expressed in μs^{-1}. After calculation, q values of 0.3, 0.1, 0.7, 0.9 are obtained for Dy-*cis*-DOTA-BC_{12}PheA, Dy-*cis*-DOTA-BC_{14}PheA, Dy-*trans*-DOTA-BC_{12}PheA, and Dy-*trans*-DOTA-BC_{14}PheA respectively. It has been previously reported that the non-ionic surfactant Tween 80® at the periphery of the assembled structures is able to form hydrogen bonds with H_2O and act as a competitor in lanthanide coordination, resulting in a q value of less than 1. As a result, less non-radiative deactivation due to O–H vibrations will take part, leading to longer luminescence lifetimes. This is reflected by a reduced q number found by the phenomenological eqn (1).[30,46,47,55–58] The observed variation in q values between *cis*- and *trans*-orientation is an identical pattern which was also observed with Tb(III) micelles based on this amphiphilic chelator, however, we speculate that the larger Tb(III) ion allows for slightly higher q values.[47] The difference in substituent orientation in *cis*- and *trans*-DOTA ligands most likely results in different "packing" into the DPPC micelle causing different values of q.

Dy(III) luminescence quantum yields of all micelles were determined by excitation at 265 nm into the ligand levels. Values of 0.8, 0.7, 0.6, and 0.6% have been calculated for Dy-*cis*-DOTA-BC_{12}PheA, Dy-*cis*-DOTA-BC_{14}PheA, Dy-*trans*-DOTA-BC_{12}PheA, and Dy-*trans*-DOTA-BC_{14}PheA respectively. These quantum yields are slightly lower compared to Dy-DTPA-BC_nPheA[46] which is most likely due to the larger q values found in Dy–DOTA derivatives (Table 1). The variation in the quantum yields appears to correspond to the varying values of q between the same orientations. The increased water coordination around lanthanide ion provides more quenching of luminescence. However, the quantum yields values are in the similar range compared to other reported dysprosium micelles.[59,60]

Table 1 Photophysical data for the Dy(III) micelles in water (pH 7.4, 0.1 wt%) at 298 K

Complex	τ H_2O[a] [μs]	τ D_2O[a] [μs]	q H_2O	Q^L_{Dy}[b] [%]
DTPA-BC_{12}[c]	26.7	115.1	0.0	0.9
DTPA-BC_{14}[c]	28.2	188.6	0.1	1.1
cis-DOTA-BC_{12}	14.9	39.5	0.3	0.8
cis-DOTA-BC_{14}	17.5	41.4	0.1	0.7
trans-DOTA-BC_{12}	11.1	34.0	0.7	0.6
trans-DOTA-BC_{14}	10.1	32.6	0.9	0.6

[a] Average of three measurements which vary by no more than 0.2 μs. [b] Estimated relative errors Q^L_{Dy} ± 10%. Quantum yields relative to rhodamine 101 in EtOH. [c] From ref. 46.

Relaxometric studies

Proton longitudinal relaxation rate. The enhancement of the relaxation rate by 1 mM of the Dy(III) compound determines the proton longitudinal relaxivity (r_1). In Fig. 4, the proton longitudinal relaxivities of the four compounds at 20, 60, 300, and 500 MHz are depicted. It can be seen that the profiles of the four compounds all follow the same trend. At low magnetic fields (20–60 MHZ), low r_1 values of 0.14–0.41 mM^{-1} s^{-1} are obtained. At higher magnetic fields (300–500 MHz), a slight increase of r_1 to 0.68 mM^{-1} s^{-1} is observed. The different values of r_1 observed between the different micelles are most likely due to combination of their different value of q and different packing efficiency within the micellar structure.

Both inner- ($1/T_1^{is}$) and outer-sphere ($1/T_1^{os}$) contributions to the proton longitudinal relaxation rate are defined by the sum of dipolar ($1/T_1^{DD}$) and Curie ($1/T_1^{C}$) contributions. At low magnetic fields, the longitudinal relaxation rate is mainly modulated by the dipolar interactions between the water proton nuclei and the static magnetic moment arising from the electrons of Dy(III), being highly dependent on the electronic relaxation time τ_S.[39,42] Those findings explain the low r_1 values in this region since Dy(III) is characterized by very short τ_S (~0.5 ps).[39,61,62] At high magnetic fields, the Curie inner- and outer-sphere contributions become more significant. These terms are modulated by the rotational correlation time of the compound τ_R and the translational correlation time τ_D; τ_D equals a^2/D, in which a is the distance of the closest approach between the water protons and the paramagnetic centre, and D is the relative diffusion constant of the water molecules and the complex. The proton longitudinal relaxivity will thus slightly increase at higher fields.

Previously reported Gd(III) complexes forming the micelle morphology have exhibited rather different frequency dependence of r_1 values whereby with increasing frequency, r_1 values

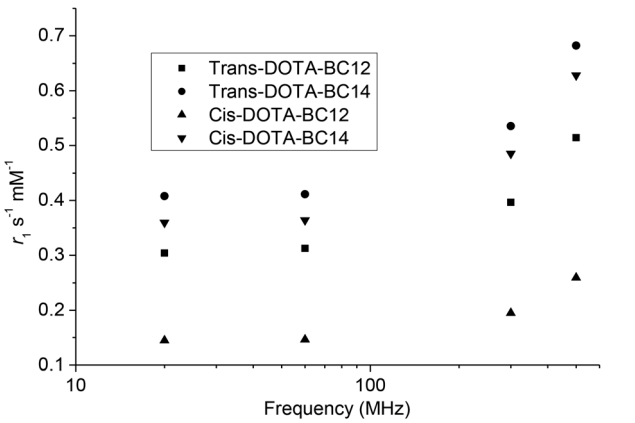

Fig. 4 Proton longitudinal relaxivity of the micelles *versus* proton Larmor frequency at 310 K.

slightly decreased to reach a plateau value until 200 MHz.[63] Contrary to Gd(III), the paramagnetic relaxation of Dy(III) complexes are quite different. For Gd(III) complexes, the main contributions to the water proton relaxation rates are: firstly, the dipolar inner sphere interaction modulated by (i) the electronic relaxation times of Gd(III); the values are usually larger than 80 ps at low field and increase with the magnetic field; (ii) the rotational correlation time that depends on the size of the complex or the size of the structure in which the Gd(III) complex is embedded; (iii) on the water residence time which is usually larger than 10 ns. Secondly, the dipolar outer sphere interaction modulated by the electronic relaxation time and the diffusion correlation time.

The concentrations of *trans*-DOTA-BC_{12}, *trans*-DOTA-BC_{14}, *cis*-DOTA-BC_{12}, *cis*-DOTA-BC_{14} were 8.11, 9.19, 5.34, 6.81 mM respectively measured by total reflection X-ray fluorescence.

For Dy(III) complexes, the dipolar contribution to the inner sphere mechanism is very low because of the fast and field independent electronic relaxation rate (smaller than 1 ps). This explains the very low relaxation rate observed at low magnetic fields. In addition to this dipolar contribution, a Curie contribution has to be taken into account. This contribution depends on <Sz> and thus on the magnetic field and is modulated by the rotational correlation time and the water residence time. This contribution becomes important only at high magnetic field due to the field dependence of <Sz>. This explains the shape of the NMRD curve obtained for the longitudinal relaxivity which remains very low as compared to Gd(III) complexes in analogous structures.

Proton transverse relaxation rate. Fig. 5 depicts the T_2 enhancement at 20, 60, 300, and 500 MHz by the Dy micelles. At the proton Larmor frequency of 20 MHz, the transverse relaxivities for the micelles are slightly higher in comparison to the longitudinal values (r_2 = 0.23–0.48 mM^{-1} s^{-1}). This increase is most likely due to the aggregation of the complexes into micelles.

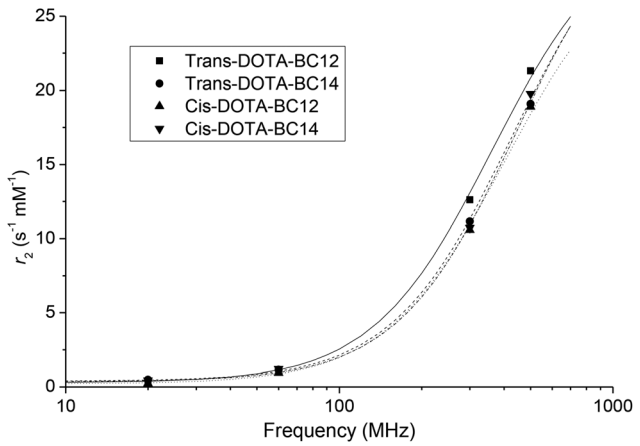

Fig. 5 Proton transverse relaxivity of the micelles *versus* proton Larmor frequency at 310 K. The lines represent the fitted data.

At higher magnetic fields (ν_o > 100 MHz), a significant increase of r_2 takes place. It is known that transverse relaxivity depends on the square of the magnetic field, despite this r_2 shows a strong reliance to the τ_M value when the external magnetic field is increased. In that particular case, it is important that the chemical shift difference between coordinated and bulk water ($\Delta\omega_M$) remains low compared with the water exchange rate.[39] The chemical shift of the coordinated water molecule is proportional to the magnetic field and is the sum of contact and pseudo-contact terms.

Fitting of the data is performed using the equations defining the inner- and outer-sphere contributions as described by Vander Elst *et al.*[39] The inner-sphere contributions depends on the ratio of [Dy complex]/[water], the value of q, the water residence time τ_M and the transverse relaxation rate of the coordinated water molecule, $1/T_{2M}$. The latter factor results from dipolar, dipolar Curie, and Curie contact contributions. The correlation time τ_C modulating the dipolar interaction, is related to τ_R, τ_S, and τ_M through $\tau_C^{-1} = \tau_R^{-1} + \tau_S^{-1} + \tau_M^{-1}$ whereas the Curie contribution is modulated by $\tau_{CC}^{-1} = \tau_R^{-1} + \tau_M^{-1}$. During the fitting procedure, the parameters q = bound water molecules(s) as determined by luminescence lifetimes, r = 0.31 nm, a = 0.36 nm, $D = 3.3 \times 10^{-9}$ m^2 s^{-1} and τ_R = 1 ns were fixed. The parameters τ_S, τ_M and $\Delta\omega_M$ are extracted from the fitting and are listed in Table 2 but they should only be considered as estimates as the fitting is only over 4 points. The τ_S values lie in the range of 0.2–0.7 ps. Fitting the proton nuclear magnetic relaxation dispersion (NMRD) profiles of the micelles shows similar correlation with our previously reported Tb(III) micelles where the q value for *trans*-DOTA is greater that of *cis*-DOTA.[47] Again, the *trans*-orientation shows double the water residence time (τ_M) of the *cis*-orientation. Furthermore, the q values of the Dy(III)–DOTA complexes are lower than Tb(III)–DOTA which could be explained by the decrease in atomic radius leading to less space for water to coordinate. Despite a reduction of the luminescence quenching effect induced by interactions of Tween 80®, a certain amount of coordinated water molecules can still be monitored by MR measurements.

The slow molecular motion leads to transverse relaxivities of 18.9, 19.8, 21.3, and 19.1 mM^{-1} s^{-1} for Dy-*cis*-DOTA-BC_{12}PheA, Dy-*cis*-DOTA-BC_{14}PheA, Dy-*trans*-DOTA-BC_{12}PheA, and Dy-*trans*-DOTA-BC_{14}PheA respectively at 11.7 T.

Table 2 Values of τ_S, τ_M, and $\Delta\omega_M$ obtained by fitting of the ^1H r_2 data of the Dy(III) micelles at 310 K

Complex	τ_s [ps]	τ_M [ns]	$\Delta\omega_M$ [10^5 rad s^{-1} T^{-1}]
DTPA-BC_{12} [e]	0.3	100	4.0[b]/5.4[c]
DTPA-BC_{14} [e]	0.3	100	3.9[b]/7.5[d]
cis-DOTA-BC_{12}	0.4	180	5.9
cis-DOTA-BC_{14}	0.7[a]	160	6.0
trans-DOTA-BC_{12}	0.5	400	2.9
trans-DOTA-BC_{14}	0.65	460	2.2

τ_R is fixed at 1000 ps. [a] q = 0.3 as q = 0.1 seems unrealistic. [b] Fitting value with q set to 1. [c] q set to 0.4. [d] q set to 0.6. [e] From ref. 46.

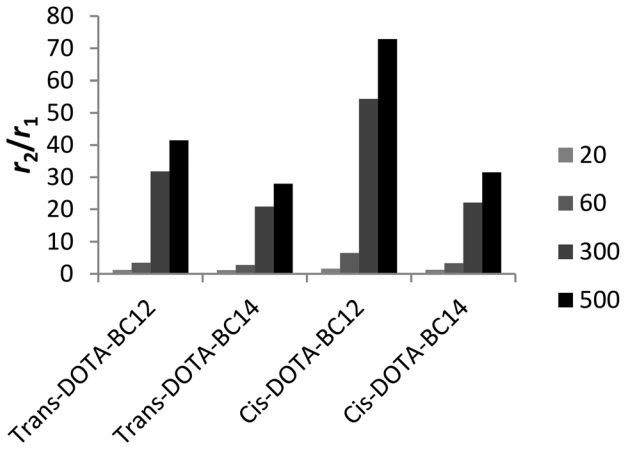

Fig. 6 Ratio of proton transverse *versus* longitudinal relaxivity at 20, 60, 300 and 500 MHz for the Dy(III) micelles at 310 K.

The Curie spin relaxation is prevailingly expressed as an inner-sphere effect. The compounds performing as efficient r_2 agents are enforced by the high magnetic moment of the dysprosium ion ($\mu = 10.2\mu_B$), the presence of a water molecule in the first coordination sphere, and long rotational correlation time.[42] Furthermore, it has been reported that DPPC forms micelles of 50 phospholipid molecules[64] in which the Dy(III) load will be equal to 4 molecules per micelle. This makes a per-particle expression possible, which equals 75.6, 79.2, 85.2, and 76.4 micelle per s for Dy-*cis*-DOTA-BC_{12}PheA, Dy-*cis*-DOTA-BC_{14}PheA, Dy-*trans*-DOTA-BC_{12}PheA, and Dy-*trans*-DOTA-BC_{14}PheA respectively.

Contrast agents with significant r_2/r_1 ratios can be beneficial because tissues display a shorter T_2 than T_1 by using appropriate pulse sequences in clinical applications. The r_2/r_1 ratios for the Dy micelles are depicted in Fig. 6, which shows that this ratio increases for all micelles with increasing magnetic field strength. The largest ratio of r_2/r_1 is observed with Dy-*cis*-DOTA-BC_{12}PheA which is explainable by the very low r_1 values that arises from a low value of q.

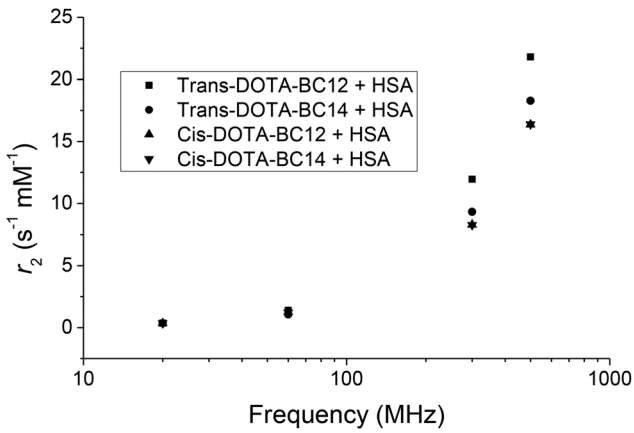

Fig. 7 Proton transverse relaxivity of the micelles with HSA 4 wt% *versus* proton Larmor frequency at 310 K. The concentrations of *trans*-DOTA-BC12+HSA, *trans*-DOTA-BC14, *cis*-DOTA-BC12, *cis*-DOTA-BC14 were 7.57, 8.27, 8.10, 8.05 mM respectively measured by total reflection X-ray fluorescence.

Micelle stability

To gain some insight into the stability of the micellar contrast agents, the solutions were incubated in sealed vials at 37 °C and analysed on a 24 hourly basis for 1 week by DLS. There was no aggregate formation observed and the micelles remain monodispersed in aqueous solution (E.S.I).

Additionally, interaction between the micelles with human serum albumin (HSA), which is the most abundant protein in plasma was studied. After incubating the micelles with 4 wt% of HSA in water at 37 °C, there was very little change in the relaxivity, which suggest that the micelles remain stable in presence of HSA and show little or no interaction with HSA that influences relaxation properties (Fig. 7).

Conclusions

Amphiphilic dysprosium(III) complexes built into mixed micelles reported in this study show favourable magnetic and optical properties, making them potential candidates for MR and optical imaging. The micelles showed long luminescence lifetimes in H_2O at the emission wavelength of 576 nm and quantum yields exceeding 0.5%. The micelles also exhibit high transverse relaxivities, r_2, all reaching around 20 s^{-1} mM^{-1} at 500 MHz and 310 K, which is a large increase when comparing with an r_2 value of 0.8 s^{-1} mM^{-1} for Dy–DTPA.[39] The increased transverse relaxivity is mainly due to the increase of the rotational correlation time especially at high magnetic fields. By using the macrocyclic DOTA chelator, smaller mono-disperse micelles were obtained in comparison to the analogous DTPA complexes. Smaller micelles are advantageous when taking bio-compatibility and elimination from the body into account, and in this work we have achieved mono-disperse micelles ranging from 10–15 nm in diameter. The micelles are stable and remain monodisperse when incubated at 37 °C for 4 days. Compared to recently reported Tb(III) micelles, the Dy(III) micelles exhibit nearly 25% increase in transverse relaxivity. However as Dy(III) complexes typically show lower quantum yield, a trade-off in performance has to be considered when finding the bimodal probe which is best balanced to address the sensitivities of both imaging techniques.

Experimental

Materials

Reagents and solvents were obtained from Sigma-Aldrich (Bornem, Belgium), Acros Organics (Geel, Belgium), ChemLab (Zedelgem, Belgium), Matrix Scientific (Columbia, USA) and BDH Prolabo (Leuven, Belgium), and were used without further purification. Dysprosium(III) chloride hexahydrate was obtained from Sigma-Aldrich (Bornem, Belgium).

Instrumentation

^{1}H spectra were recorded by using a Bruker Avance 300 spectrometer (Bruker, Karlsruhe, Germany), operating at 300 MHz for ^{1}H.

IR spectra were measured by using a Bruker Vertex 70 FT-IR spectrometer (Bruker, Ettlingen, Germany).

ESI-Mass spectra were obtained by using a Thermo Finnigan LCQ Advantage mass spectrometer. Samples for the mass spectrometry were prepared by dissolving the product (2 mg) in methanol (1 mL), then adding 200 μL of this solution to a water/methanol mixture (50 : 50, 800 μL). The resulting solution was injected at a flow rate of 5 μL min^{-1}.

Accurate mass spectra were acquired on a quadrupole orthogonal acceleration time-of-flight mass spectrometer (Synapt G2 HDMS, Waters, Milford, MA). Samples were infused at 3 μL min^{-1} and spectra were obtained in positive ionization mode with a resolution of 15 000 (FWHM) using leucine enkephalin as lock mass.

TXRF measurements were performed on a Bruker S2 Picofox (Bruker, Berlin, Germany) with a molybdenum source. Dysprosium(III) solutions of approximately 1000 ppm in milli-Q water were prepared and 500 μL of this solution was mixed with 500 μL of a 1000 ppm Chem-Lab gallium standard solution (1000 μg mL^{-1}, 2–5% HNO_3). 10 μL of this mixture with similar Dy(III)–Ga(III) concentrations was put on a Bruker AXS quartz glass sample plate for measurement.

Solutions were dispersed in a 180 W Bandelin Sonorex RK 510 H sonicator equipped with a thermostatic heating bath.

Absorption spectra were measured on a Varian Cary 5000 spectrophotometer on freshly prepared aqua solutions in quartz Suprasil cells (115F-QS) with an optical pathlength of 1 cm.

Emission spectra and luminescence decays of Dy(III) complexes were recorded on an Edinburgh Instruments FS920 steady state spectrofluorimeter. This instrument is equipped with a 450 W xenon arc lamp, a high energy microsecond flashlamp mF900H and an extended red-sensitive photomultiplier (185–1010 nm, Hamamatsu R 2658P). All spectra are corrected for the instrumental functions. Luminescence decays were determined under ligand excitation (270–280 nm) monitoring emission of the $^4F_{9/2} \rightarrow {}^6H_{13/2}$ transition for Dy(III) complexes. Luminescence decays were analyzed using Edinburgh software; lifetimes are averages of at least three measurements. Quantum yields were determined by a comparative method with a standard reference; estimated experimental errors for quantum yield determination ±10%. Rhodamine 101 (Sigma) in ethanol (Q = 100%) was used as a standard for the complexes. Solutions with a concentration of about 10^{-5} M were prepared to obtain an optical density lower than 0.05 at the excitation wavelength.

Relaxometry

^{1}H T_1 and T_2 measurements were performed at 310 K at 0.47, 1.41, 7.05, and 11.75 T on Minispec mq-20, mq-60, Avance-300 and Avance-500 from Bruker, respectively. T_1 were measured using the inversion–recovery sequence and T_2 were obtained using CMPG sequence. The echo time was set to 1 ms. The diamagnetic contribution was the contribution of pure water.

DLS measurements

Photon correlation spectroscopy was performed at room temperature with a BIC multiangle laser light-scattering system with a 90° scattering angle (Brookhaven Instruments Corporation, Holtsville, USA). The intensity weighted micellar diameter was measured on 0.01 wt% diluted suspensions in Milli-Q water, sonicated for 15 min, passed through a 200 nm PTFE filter before analysis and calculated by a non-negatively constrained least-squares (multiple pass) routine.

Synthesis

Chloroacetamides, *cis*-DOTA-BC$_{12}$PheA, *cis*-DOTA-BC$_{14}$PheA, *trans*-DOTA-BC$_{12}$PheA, and *trans*-DOTA-BC$_{14}$PheA and complexes.

2-Chloro-*N*-(4-dodecylphenyl)acetamide and 2-chloro-*N*-(4-tetradecylphenyl)acetamide. 4-Dodecyaniline (1 g, 3.82 mmol, 1 eq.) or 4-tetradecyaniline (1 g, 3.45 mmol, 1 eq.) were dissolved in dichloromethane (10 mL) and potassium carbonate (1.32 g or 1.19 g, 9.56 mmol or 8.64 mmol, 2.5 eq.) was added and the suspension was stirred for 30 minutes at ambient temperature. Chloroacetyl chloride (0.457 g or 0.429 g, 4.21 mmol or 3.80 mmol, 1.1 eq.) was slowly added and mixed for 10 minutes. The reaction was held at reflux for 4 hours then allowed to cool to ambient temperature, after which the filtrate was concentrated to obtain a residue which was recrystallized in hexane to afford the final product.

2-Chloro-*N*-(4-dodecylphenyl)acetamide. Yield: 1.15 g, 89%; ^{1}H NMR (300 MHz, CD_2Cl_2, 25 °C, TMS): δ = 0.91 (t, 3H, C**H**$_3$-(CH$_2$)$_9$-CH$_2$-CH$_2$-Ar), 1.30, 1.32 (m, 18H, CH$_3$-(C**H**$_2$)$_9$-CH$_2$-CH$_2$-Ar), 1.62 (m, 2H, CH$_3$-(CH$_2$)$_9$-C**H**$_2$-CH$_2$-Ar), 2.62 ppm (t, 2H, CH$_3$-(CH$_2$)$_9$-CH$_2$-C**H**$_2$-Ar), 4.21 (s, 2H, Cl-C**H**$_2$-CO), 7.19, 7.22 (d, 2H, phenyl C**H**), 7.45, 7.48 (d, 2H, phenyl 2 × C**H**), 8.16 ppm (s, 1H, amide N**H**). ESI-MS (+ve mode): m/z: calcd 360.9 [M + Na]$^+$, found 363.0 [M + Na]$^+$, 699.8 [2M + Na]$^+$.

2-Chloro-*N*-(4-tetradecylphenyl)acetamide. Yield: 0.64 g, 51%; ^{1}H NMR (300 MHz, CD_2Cl_2, 25 °C, TMS): δ = 0.91 (t, 3H, C**H**$_3$-(CH$_2$)$_{11}$-CH$_2$-CH$_2$-Ar), 1.29, 1.34 (m, 22H, CH$_3$-(C**H**$_2$)$_{11}$-CH$_2$-CH$_2$-Ar), 1.62 (m, 2H, CH$_3$-(CH$_2$)$_{11}$-C**H**$_2$-CH$_2$-Ar), 2.62 ppm (t, 2H, CH$_3$-(CH$_2$)$_{11}$-CH$_2$-C**H**$_2$-Ar), 4.21 (s, 2H, Cl-C**H**$_2$-CO), 7.19, 7.22 (d, 2H, phenyl C**H**), 7.45, 7.48 (d, 2H, phenyl 2 × C**H**), 8.16 ppm (s, 1H, amide N**H**). ESI-MS (+ve mode): m/z: calcd 389.0 [M + H]$^+$, found 391.1 [M + Na]$^+$, 754.1 [2M + Na]$^+$.

cis-DOTA-BC$_{12/14}$PheA

Di-*tert*-butyl 2,2′-(1,4,7,10-tetraazacyclododecane-1,4-diyl) diacetate. 1,4,7,10-Tetraazacyclododecane (1 g, 5.63 mmol, 1 eq.) was dissolved in anhydrous chloroform (80 mL), placed under an argon atmosphere, DIPEA (1.819 g, 14.1 mmol, 2.5 eq.) was added, and the solution was mixed for 15 minutes. *tert*-Butyl bromoacetate (2.197 g, 11.3 mmol, 2 eq.) mixed in chloroform (20 mL) was added slowly for approximately 30 minutes and the reaction was allowed to continuously stir

for a further 12 hours. The resulting solution was washed with water (3 × 60 mL) and the organic phase dried over Mg_2SO_4. The solvent was removed and crude product was purified by column chromatography (basic Al_2O_3, dicholoromethane/methanol, 98 : 2) to afford the final colourless oily compound (0.87 g, 39%).

^{1}H NMR (300 MHZ, $CDCl_3$, 25 °C, TMS): δ = 1.46 (s, 18H, 2 × (C**H**$_3$)$_3$-O-CO), 2.7 (m, 4H, O-CO-N-(CH$_2$)$_2$-N-(C**H**$_2$)$_2$-N-(CH$_2$)$_2$-N-CO-O), 2.78 (m, 12H, O-CO-CH$_2$-N-(C**H**$_2$)$_4$-(2×)C**H**$_2$-CH$_2$-N), 3.32 ppm (m, 4H, O-CO-C**H**$_2$-N). ESI-MS (+ve mode): *m*/*z*: calcd 401.6 $[M + H]^+$, found 401.6 $[M + H]^+$, 423.8 $[M + Na]^+$.

Di-*tert*-butyl 2,2′-(7,10-bis(2-((4-dodecylphenyl)amino)-2-oxoethyl)-1,4,7,10-tetraazacyclododecane-1,4-diyl)diacetate (protected-*cis*-DOTA-BC12PhenA) and di-*tert*-butyl 2,2′-(7,10-bis(2-oxo-2-((4-tetradecylphenyl)amino)ethyl)-1,4,7,10-tetraazacyclododecane-1,4-diyl)diacetate (protected-*cis*-DOTA-BC14PheA). Di-*tert*-butyl 2,2′-(1,4,7,10-tetraazacyclododecane-1,4-diyl)diacetate (0.23 g, 0.57 mmol, 1 eq.) was dissolved in dry acetonitrile (15 mL) and potassium carbonate (0.397 g, 2.87 mmol, 5 eq.) was added with the suspension being heated to reflux. 2-Chloro-*N*-(4-dodecylphenyl)acetamide (0.485 g, 1.44 mmol, 2.5 eq.) or 2-chloro-*N*-(4-tetradecylphenyl)acetamide (0.525 g, 1.44 mmol, 2.5 eq.) was dissolved in warm acetonitrile (50 mL), added drop-wise and the reaction was held at reflux for 48 hours. After allowing the suspension to cool to ambient temperature, the potassium carbonate was separated by filtration and the solvent was removed. The crude product was purified by column chromatography (neutral Al_2O_3, dichloromethane/methanol, 98 : 2) to afford the final colourless oily product.

Protected-cis-DOTA-BC$_{12}$PhenA. Yield: 0.31 g, 54%; ^{1}H NMR (300 MHz, $CDCl_3$, 25 °C, TMS): δ = 0.88 (t, 6H, 2 × C**H**$_3$-(CH$_2$)$_{10}$-CH$_2$-Ar), 1.26 (m, 40H, 2 × C**H**$_3$-(C**H**$_2$)$_{10}$-CH$_2$-Ar), 1.40 (s, 18H, 2 × (C**H**$_3$)$_3$-O-CO), 2.55 (t, 4H, 2 × C**H**$_3$-(CH$_2$)$_{10}$-C**H**$_2$-Ar), 2.77, 2.81, 2.87 (m, 12H, DOTA 4 × C**H**$_2$), 3.01 (m, 4H, O-CO-N-(C**H**$_2$)$_2$-N-CO-O), 3.18 (m, 4H, 2 × N-C**H**$_2$-CO-NH), 3.26 (m, 4H, 2 × N-C**H**$_2$-CO-O), 7.06, 7.09 (d, 4H, phenyl 4 × C**H**), 7.46, 7.49 (d, 4H, phenyl 4 × C**H**), 9.49 ppm (s, 2H, amide 2 × N**H**). ESI-MS (+ve mode): *m*/*z*: calcd 1026.5 $[M + Na]^+$, found 1026.4 $[M + Na]^+$.

Protected-cis-DOTA-BC$_{14}$PhenA. Yield: 0.35 g, 57%; ^{1}H NMR (300 MHz, $CDCl_3$, 25 °C, TMS): δ = 0.87 (t, 6H, 2 × C**H**$_3$-(CH$_2$)$_{12}$-CH$_2$-Ar), 1.26 (m, 44H, 2 × C**H**$_3$-(C**H**$_2$)$_{12}$-CH$_2$-Ar), 1.40 (s, 18H, 2 × (C**H**$_3$)$_3$-O-CO), 2.54 (t, 4H, 2 × C**H**$_3$-(CH$_2$)$_{12}$-C**H**$_2$-Ar), 2.77, 2.81, 2.87 (m, 12H, DOTA 6 × C**H**$_2$), 3.01 (m, 4H, O-CO-N-(C**H**$_2$)$_2$-N-CO-O), 3.18 (m, 4H, N-C**H**$_2$-CO-NH), 3.26 (m, 4H, 2 × N-C**H**$_2$-CO-O), 7.06, 7.09 (d, 4H, phenyl 4 × C**H**), 7.46, 7.49 (d, 4H, phenyl 4 × C**H**), 9.49 ppm (s, 2H, amide 2 × N**H**). ESI-MS (+ve mode): *m*/*z*: calcd 1082.6 $[M + Na]^+$, found 1084.1 $[M + Na]^+$.

2,2′-(7,10-Bis(2-((4-dodecylphenyl)amino)-2-oxoethyl)-1,4,7,10-tetraazacyclododecane-1,4-diyl)diacetic acid (*cis*-DOTA-BC$_{12}$PhenA) and 2,2′-(7,10-bis(2-((4-tetradecylphenyl)amino)-2-oxoethyl)-1,4,7,10-tetraazacyclododecane-1,4-diyl)diacetic acid (*cis*-DOTA-BC$_{14}$PhenA). Di-*tert*-butyl 2,2′-(7,10-bis(2-((4-dodecylphenyl)amino)-2-oxoethyl)-1,4,7,10-tetraazacyclododecane-1,4-diyl)diacetate (0.3 g, 0.3 mmol) or di-*tert*-butyl 2,2′-(7,10-bis(2-oxo-2-((4-tetradecylphenyl)amino)ethyl)-1,4,7,10-tetraazacyclododecane-1,4-diyl)diacetate (0.3 g, 0.28 mmol) was dissolved in dichloromethane (5 mL), trifluoroacetic acid (5 mL) was added and mixed at ambient temperature for 12 hours. Dichloromethane (5 mL) was added and the solvents removed, followed by adding at additional amount of dichloromethane (5 mL) and solvents removed a second time affording the final colourless oily product.

cis-DOTA-BC$_{12}$PhenA. Yield: quantitative; ^{1}H NMR (300 MHz, pyridine-D$_5$, 25 °C, TMS): δ = 0.89 (t, 6H, 2 × C**H**$_3$-(CH$_2$)$_9$-CH$_2$-CH$_2$-Ar), 1.27 (m, 36H, 2 × C**H**$_3$-(C**H**$_2$)$_9$-CH$_2$-CH$_2$-Ar), 1.58 (m, 4H, 2 × C**H**$_3$-(CH$_2$)$_9$-C**H**$_2$-CH$_2$-Ar), 2.55 (t, 4H, 2 × C**H**$_3$-(CH$_2$)$_9$-CH$_2$-C**H**$_2$-Ar), 3.38 (m, 16H, 8 × DOTA C**H**$_2$), 4.12 (m, 4H, 2 × N-C**H**$_2$-CO-NH), 4.27 (m, 4H, 2 × N-C**H**$_2$-CO-O), 7.16, 7.19 (d, 4H, phenyl 4 × C**H**), 8.09, 8.06 (d, 4H, phenyl 4 × C**H**), 11.42 ppm (s, 2H, amide 2 × N**H**). FT-IR: $\tilde{\nu}_{max}$ = 1626 (C═O free acid), 1529 cm^{-1} (C═O amide). ESI-MS (+ve mode): *m*/*z*: calcd 914.3 $[M + Na]^+$, found 914.2 $[M + Na]^+$.

cis-DOTA-BC$_{14}$PhenA. Yield: quantitative; ^{1}H NMR (300 MHz, pyridine-D$_5$, 25 °C, TMS): δ = 0.88 (t, 6H, CH3-(CH2)$_{11}$-CH$_2$-CH$_2$-Ar), 1.29 (m, 42H, 2 × C**H**$_3$-(C**H**$_2$)$_{11}$-CH$_2$-CH$_2$-Ar), 1.59 (m, 4H, 2 × C**H**$_3$-(CH$_2$)$_{11}$-C**H**$_2$-CH$_2$-Ar), 2.55 (t, 4H, 2 × C**H**$_3$-(CH$_2$)$_{11}$-CH$_2$-C**H**$_2$-Ar), 3.36 (m, 16H, 8 × DOTA C**H**$_2$), 4.11 (m, 4H, 2 × N-C**H**$_2$-CO-NH), 4.25 (m, 4H, 2 × N-C**H**$_2$-CO-O), 7.17, 7.20 (d, 4H, phenyl 4 × C**H**), 8.07, 8.09 (d, 4H, phenyl 4 × C**H**), 11.40 ppm (s, 2H, amide 2 × N**H**). FT-IR: $\tilde{\nu}_{max}$ = 1626 (C═O free acid), 1529 cm^{-1} (C═O amide). ESI-MS (+ve mode): *m*/*z*: calcd 970.4 $[M + Na]^+$, found 971.4 $[M + Na]^+$.

trans-DOTA-BC$_{12/14}$PheA

4,10-Bis((benzyloxy)carbonyl)-4,10-diaza-1,7-diazoniacyclododecane-1,7-diium chloride. 1,4,7,10-Tetraazacyclododecane (1 g, 5.8 mmol, 1 eq.) was dissolved in chloroform (40 mL) in an ice-bath and benzyl chloroformate (1.98 g, 11.61 mmol, 2 eq.) in chloroform (10 mL) was added drop-wise. The solution was allowed to warm to ambient temperature and mixing continued for 24 hours. The solvent was evaporated and the product suspended in diethyl ether (10 mL), filtered and washed with diethyl ether (2 × 10 mL). The solid was dried to afford a white powder (quantitative yield).

^{1}H NMR (300 MHZ, D_2O, 25 °C, TMS): δ = 3.07 (m, 8H, 2 × C**H**$_2$-NH$_2$-C**H**$_2$), 3.50 (m, 8H, 2 × C**H**$_2$-NCO$_2$-C**H**$_2$), 5.07 (s, 4H, 2 × O-CH$_2$-Ar), 7.33 ppm (m, 10H, phenyl 10 × C**H**). ESI-MS (+ve mode): *m*/*z*: calcd 441.5 $[M + H]^+$, found 441.8 $[M + H]^+$.

Dibenzyl 4,10-bis(2-(*tert*-butoxy)-2-oxoethyl)-1,4,7,10-tetraazacyclododecane-1,7-dicarboxylate. 4,10-Bis((benzyloxy)carbonyl)-4,10-diaza-1,7-diazoniacyclododecane-1,7-diium chloride (1 g, 1.95 mmol, 1 eq.) was suspended in acetonitrile (20 mL) and DIPEA (1.259 g, 9.74 mmol, 5 eq.) mixed in acetonitrile (8 mL) was added turning the solution clear. *tert*-Butyl bromoacetate (1.14 g, 5.84 mmol, 3 eq.) was mixed in acetonitrile (4 mL) and added. The solution was heated at 60 °C for 12 hours and then allowed to cool to ambient temperature. The solvent was evaporated and the residue extracted with diethyl ether (20 mL) and water (20 mL). The organic layer was

washed further with water (10 mL), sodium hydroxide solution (0.5 g/10 mL) and water (10 mL). The organic layer was dried over Mg_2SO_4 and solvent evaporated. The crude product was purified by column chromatography (neutral Al_2O_3, dichloromethane/methanol, 98 : 2) to afford the final colourless oily compound (1.1 g, 84%).

^{1}H NMR (300 MHZ, $CDCl_3$, 25 °C, TMS): δ = 1.43 (s, 18H, 2 × CO-O-C-(C**H**$_3$)$_3$), 2.87 (m, 8H, 2 × C**H**$_2$-N-C**H**$_2$), 3.13 (s, 4H, 2 × N-C**H**$_2$-CO-O), 3.42 (m, 8H, 2 × C**H**$_2$-NCOO-C**H**$_2$), 5.13 (s, 4H, 2 × CO-O-C**H**$_2$-Ar), 10.02 ppm (m, 10H, phenyl 10 × C**H**). ESI-MS (+ve mode): *m*/*z*: calcd 669.8 $[M + H]^+$, found 669.7 $[M + H]^+$.

Di-*tert*-butyl 2,2′-(1,4,7,10-tetraazacyclododecane-1,7-diyl) diacetate. Dibenzyl 4,10-bis(2-(*tert*-butoxy)-2-oxoethyl)-1,4,7,10-tetraazacyclododecane-1,7-dicarboxylate (1.1 g, 1.64 mmol) was dissolved in dry methanol (10 mL) in a high pressure vessel and Pd–C catalyst (5% Pd, 20 wt%, 0.218 g) was added. The vessel was placed on a Parr-aparatus, pressurised with hydrogen gas (40 p.s.i) and mixed for 12 hours. The solvents and by-products were removed under reduced pressure to afford the final oily colourless compound (quantitative yield).

^{1}H NMR (300 MHZ, $CDCl_3$, 25 °C, TMS): δ = 1.46 (s, 18H, 2 × CO-O-C-(C**H**$_3$)$_3$), 2.68 (m, 8H, 2 × C**H**$_2$-NH-C**H**$_2$), 2.87 (m, 8H, 2 × C**H**$_2$-NCH$_2$-C**H**$_2$), 3.35 ppm (s, 4H, 2 × N-C**H**$_2$-CO-O), ESI-MS (+ve mode): *m*/*z*: calcd 401.6 $[M + H]^+$, found 401.6 $[M + H]^+$, 423.8 $[M + Na]^+$.

Di-*tert*-butyl 2,2′-(4,10-bis(2-((4-dodecylphenyl)amino)-2-oxoethyl)-1,4,7,10-tetraazacyclododecane-1,7-diyl)diacetate (protected-*trans*-DOTA-BC$_{12}$PhenA) and di-*tert*-butyl 2,2′-(4,10-bis(2-oxo-2-((4-tetradecylphenyl)amino)ethyl)-1,4,7,10-tetraazacyclododecane-1,7-diyl)diacetate (protected-*trans*-DOTA-BC$_{14}$PhenA). Di-*tert*-butyl 2,2′-(1,4,7,10-tetraazacyclododecane-1,7-diyl)diacetate (0.171/0.13 g, 0.428/0.325 mmol, 1 eq.) was dissolved in dry acetonitrile (15 mL) and potassium carbonate (0.296 g, 2.138 mmol, 5 eq.) was added with the suspension being heated to reflux. 2-Chloro-*N*-(4-dodecylphenyl)acetamide (0.361 g, 1.07 mmol, 2.5 eq.) or 2-chloro-*N*-(4-tetradecylphenyl) acetamide (0.297 g, 0.812 mmol, 2.5 eq.) was dissolved in warm acetonitrile (50 mL), added drop-wise and the reaction was held at reflux for 48 hours. After allowing the suspension to cool to ambient temperature, the potassium carbonate was separated by filtration and the solvent was removed. The crude product was purified by column chromatography (neutral Al_2O_3, dichloromethane/methanol, 98 : 2) to afford the final colourless oily product.

Protected-trans-DOTA-BC$_{12}$PhenA. Yield: 0.203 g, 47%. ^{1}H NMR (300 MHZ, $CDCl_3$, 25 °C, TMS): δ = 0.88 (t, 6H, 2 × C**H**$_3$-(CH$_2$)$_9$-CH$_2$-CH$_2$-Ar), 1.25 (m, 36H, CH$_3$-(C**H**$_2$)$_9$-CH$_2$-CH$_2$-Ar), 1.36 (s, 18H, 2 × (C**H**$_3$)$_3$-O-CO), 1.62 (m, 4H, 2 × C**H**$_3$-(CH$_2$)$_9$-C**H**$_2$-CH$_2$-Ar), 2.54 (t, 4H, 2 × C**H**$_3$-(CH$_2$)$_9$-CH$_2$-C**H**$_2$-Ar), 2.81 (m, 4H, O-CO-N-(CH$_2$)$_2$-N-(C**H**$_2$)$_2$-N-(CH$_2$)$_2$-N-CO-O), 2.93 (m, 8H, O-CO-N-(C**H**$_2$)$_2$-N-(CH$_2$)$_2$-N-(C**H**$_2$)$_2$-N-CO-O), 3.19 (m, 4H, 2 × N-C**H**$_2$-CO-NH), 3.21 (m, 4H, 2 × N-C**H**$_2$-CO-O), 7.08, 7.11 (d, 4H, phenyl 4 × C**H**), 7.44, 7.47 ppm (d, 4H, phenyl 4 × C**H**). ESI-MS (+ve mode): *m*/*z*: calcd 1026.5 $[M + Na]^+$, found 1026.4 $[M + Na]^+$.

Protected-trans-DOTA-BC$_{14}$PhenA. Yield: 0.297 g, 49%. ^{1}H NMR (300 MHZ, $CDCl_3$, 25 °C, TMS): δ = 0.88 (t, 6H, 2 × C**H**$_3$-(CH$_2$)$_{11}$-CH$_2$-CH$_2$-Ar), 1.25 (m, 44H, 2 × C**H**$_3$-(C**H**$_2$)$_{11}$-CH$_2$-CH$_2$-Ar), 1.36 (s, 18H, 2 × (C**H**$_3$)$_3$-O-CO), 1.62 (m, 4H, 2 × C**H**$_3$-(CH$_2$)$_{11}$-C**H**$_2$-CH$_2$-Ar), 2.54 (t, 4H, 2 × C**H**$_3$-(CH$_2$)$_{11}$-CH$_2$-C**H**$_2$-Ar), 2.81 (m, 4H, O-CO-N-(CH$_2$)$_2$-N-(C**H**$_2$)$_2$-N-(CH$_2$)$_2$-N-CO-O), 2.93 (m, 8H, O-CO-N-(C**H**$_2$)$_2$-N-(CH$_2$)$_2$-N-(C**H**$_2$)$_2$-N-CO-O), 3.19 (m, 4H, 2 × N-C**H**$_2$-CO-NH), 3.21 (m, 4H, 2 × N-C**H**$_2$-CO-O), 7.08, 7.11 (d, 4H, phenyl 4 × C**H**), 7.44, 7.47 ppm (d, 4H, phenyl 4 × C**H**). ESI-MS (+ve mode): *m*/*z*: calcd 1082.6 $[M + Na]^+$, found 1084.1 $[M + Na]^+$.

2,2′-(4,10-Bis(2-((4-dodecylphenyl)amino)-2-oxoethyl)-1,4,7,10-tetraazacyclododecane-1,7-diyl)diacetic acid (*trans*-DOTA-BC$_{12}$PhenA) and 2,2′-(4,10-bis(2-((4-tetradecylphenyl)amino)-2-oxoethyl)-1,4,7,10-tetraazacyclododecane-1,7-diyl)diacetic acid (*trans*-DOTA-BC$_{14}$PhenA). Di-*tert*-butyl-2,2′-(4,10-bis(3-((4-dodecylphenyl)amino)-2-oxopropyl)-1,4,7,10-tetraazacyclododecane-1,7-diyl)diacetate (0.203 g, 0.197 mmol) or 2,2′-(4,10-bis(2-oxo-3-((4-tetradecylphenyl)amino)propyl)-1,4,7,10-tetraazacyclododecane-1,7-diyl)diacetic acid (0.169 g, 0.156 mmol) was dissolved in was dissolved in dichloromethane (5 mL), trifluoroacetic acid (5 mL) was added and mixed at ambient temperature for 12 hours. Dichloromethane (5 mL) was added and the solvents removed, followed by adding at additional amount of dichloromethane (5 mL) and solvents removed a second time affording the final colourless oily product.

trans-DOTA-BC$_{12}$PhenA. Yield: quantitative; ^{1}H NMR (300 MHz, pyridine-D5, 25 °C, TMS): δ = 0.91 (t, 6H, 2 × C**H**$_3$-(CH$_2$)$_9$-CH$_2$-CH$_2$-Ar), 1.32 (m, 36H, 2 × C**H**$_3$-(C**H**$_2$)$_9$-CH$_2$-CH$_2$-Ar), 1.58 (m, 4H, 2 × C**H**$_3$-(CH$_2$)$_9$-C**H**$_2$-CH$_2$-Ar), 2.54 (t, 4H, 2 × C**H**$_3$-(CH$_2$)$_9$-CH$_2$-C**H**$_2$-Ar), 3.12, 3.38 (m, 16H,DOTA 8 × C**H**$_2$), 4.07 (m, 4H, 2 × N-C**H**$_2$-CO-NH), 4.32 (m, 4H, 2 × N-C**H**$_2$-CO-O), 7.12, 7.15 (d, 4H, phenyl 4 × C**H**), 8.04, 8.07 (d, 4H, phenyl 4 × C**H**). FT-IR: $\tilde{\nu}_{max}$ = 1626 (C═O free acid), 1529 cm^{-1} (C═O amide). ESI-MS (+ve mode): *m*/*z*: calcd 914.3 $[M + Na]^+$, found 914.2 $[M + Na]^+$.

trans-DOTA-BC$_{14}$PhenA. Yield: quantitative; ^{1}H NMR (300 MHz, pyridine-D5, 25 °C, TMS): δ = 0.91 (t, 6H, 2 × C**H**$_3$-(CH$_2$)$_{11}$-CH$_2$-CH$_2$-Ar), 1.32 (m, 44H, 2 × C**H**$_3$-(C**H**$_2$)$_{11}$-CH$_2$-CH$_2$-Ar), 1.58 (m, 4H, 2 × C**H**$_3$-(CH$_2$)$_{11}$-C**H**$_2$-CH$_2$-Ar), 2.54 (t, 4H, 2 × C**H**$_3$-(CH$_2$)$_{11}$-CH$_2$-C**H**$_2$-Ar), 3.12, 3.38 (m, 16H, DOTA 8 × C**H**$_2$), 4.07 (m, 4H, 2 × N-C**H**$_2$-CO-NH), 4.32 (m, 4H, 2 × N-C**H**$_2$-CO-O), 7.12, 7.15 (d, 4H, phenyl 4 × C**H**), 8.04, 8.07 (d, 4H, phenyl 4 × C**H**). FT-IR: $\tilde{\nu}_{max}$ = 1626 (C═O free acid), 1529 cm^{-1} (C═O amide). ESI-MS (+ve mode): *m*/*z*: calcd 970.4 $[M + H]^+$, found 971.4 $[M + Na]^+$.

Dysprosium(III) *cis*-DOTA-BC$_{12}$PhenA, *cis*-DOTA-BC$_{14}$PhenA, *trans*-DOTA-BC$_{12}$PhenA, *trans*-DOTA-BC$_{14}$PhenA complexes. The ligand (0.1 g, ±0.1 mmol, 1 eq.) was dissolved in pyridine (5 mL) and a solution of hydrated $DyCl_3$ hexahydrate salt (0.11 mmol, 1.1 eq.) in H_2O (0.2 mL) was added. The mixture was brought to 70 °C for 3 hours after which the solvents were evaporated. The crude product was suspended in acetone (10 mL) and filtered over a Büchner. The solid was washed with an acetone/water 50 : 50 mixture (2 × 5 mL) to remove any free Dy(III) ions, rinsed again with acetone (2 × 10 mL) and

dried *in vacuo*. The absence of free lanthanide ions was checked with an arsenazo indicator.

Dy(III)-cis-DOTA-BC$_{12}$PhenA. Yield: 43%; IR: $\tilde{\nu}_{max}$ = 1596 (COO^- asym. stretch), 1514 (amide II), 1391 cm^{-1} (COO^- sym. stretch); ESI-MS (+ve mode): *m*/*z*: calcd 1053.6 $[M + H]^+$, found 1053.0 $[M + H]^+$; accurate mass (+ve mode): *m*/*z*: calcd 1052.5744 $[M]^+$, found 1052.5745 $[M]^+$; M.p. complex decomposes above 300 °C.

Dy(III)-cis-DOTA-BC$_{14}$PhenA. Yield: 73%; IR: $\tilde{\nu}_{max}$ = 1595 (COO^- asym. stretch), 1514 (amide II), 1392 cm^{-1} (COO^- sym. stretch); ESI-MS (+ve mode): *m*/*z*: calcd 1109.6 $[M + H]^+$, found 1108.1 $[M + H]^+$; accurate mass (+ve mode): *m*/*z*: calcd 1108.6370 $[M]^+$, found 1108.6920 $[M]^+$; M.p. complex decomposes above 300 °C.

Dy(III)-trans-DOTA-BC$_{12}$PhenA. Yield: 66%; IR: $\tilde{\nu}_{max}$ = 1595 (COO^- asym. stretch), 1514 (amide II), 1392 cm^{-1} (COO^- sym. stretch); ESI-MS (+ve mode): *m*/*z*: calcd 1053.6 $[M + H]^+$, found 1051.7 $[M + H]^+$; accurate mass (+ve mode): *m*/*z*: calcd 1052.5744 $[M]^+$, found 1052.5769 $[M]^+$; M.p. complex decomposes above 300 °C.

Dy(III)-trans-DOTA-BC$_{14}$PhenA. Yield: 63%; IR: $\tilde{\nu}_{max}$ = 1595 (COO^- asym. stretch), 1514 (amide II), 1392 cm^{-1} (COO^- sym. stretch); ESI-MS (+ve mode): *m*/*z*: calcd 1109.1 $[M + H]^+$, found 1107.9 $[M + H]^+$; accurate mass (+ve mode): *m*/*z*: calcd 1108.6370 $[M]^+$, found 1108.6356 $[M]^+$; M.p. complex decomposes above 300 °C.

Preparation of micelles

1,2-Dipalmitoyl-sn-glycero-3-phosphocholine (DPPC, 80 mg, 0.109 mmol, 12 equiv.) and the amphiphilic complex (10 mg, ±0.091 mmol, 1 equiv.) were dissolved in a 1 : 1 chloroform/methanol solution (2 mL). After evaporation of the solvents in from flask with septum and needle fitted in a vacuum oven at 50 °C, a thin film was obtained which was rehydrated with hot water (2 mL, 70 °C). To improve the solubility, the suspension was sonicated in a 180 W sonicator with a thermostatic bath at 65 °C for 15 min. Polyoxyethylene sorbitan monooleate or Tween 80® (77 mg, 0.06 mmol, 6.5 equiv.) was added as a surfactant followed by another 15 min of sonication to fulfil the process of micelle formation. Water was evaporated in a flask with septum and needle fitted in a vacuum oven overnight at 50 °C leaving a thin film. A small amount of sample was removed for DLS measurements. For preparation of samples for relaxometry measurements, the thin film was rehydrated with Milli-Q water (1 mL), sonicated for 15 min and passed through a 200 nm PTFE filter. The concentration of dysprosium(III) was analysed by TXRF before relaxometric measurements.

Acknowledgements

M.H. acknowledges the FWO Flanders (Belgium) for a doctoral fellowship. M.H. and T.P.V. thank Prof. Dr Jef Rozenski for accurate mass measurements, Laboratory of Medicinal Chemistry, Rega Institute, KU Leuven. Mass spectrometry was made possible by the support of the Hercules Foundation of the Flemish Government (grant 20100225-7). L.V.E. and S.L. thank the ARC Programs of the French Community of Belgium, the FNRS (Fonds National de la Recherche Scientifique), the UIAP VII program, the support and sponsorship concerted by COST Actions (TD1004), and the Center for Microscopy and Molecular Imaging (CMMI, supported by the European Regional Development Fund and the Walloon Region).

Notes and references

1 P. Caravan, J. J. Ellison, T. J. McMurry and R. B. Lauffer, *Chem. Rev.*, 1999, **99**, 2293–2352.
2 J. C. Hebden, S. R. Arridge and D. T. Delpy, *Phys. Med. Biol.*, 1997, **5**, 825–840.
3 F. Hu, *Nanoscale*, 2012, **4**, 6235.
4 S. L. Jeon, M. K. Chae, E. J. Jang and C. Lee, *Chem. – Eur. J.*, 2013, **19**, 4217–4222.
5 F. Ye, *Contrast Media Mol. Imaging*, 2012, **7**, 460–468.
6 S. Soenen, *Contrast Media Mol. Imaging*, 2009, **2009**, 207–219.
7 H. B. Na, I. C. Song and T. Hyeon, *Adv. Mater.*, 2009, **21**, 2133–2148.
8 J. Taubert, G. V. Belle, W. Vanduffel, B. Rossion and R. Vogels, *J. Neurosci.*, 2015, **35**, 9872–9878.
9 A. J. L. Villaraza, A. Bumb and M. W. Briechbiel, *Chem. Rev.*, 2010, **110**, 2921–2959.
10 P. Lebdušková, J. Kotek, P. Hermann, L. Vander Elst, R. N. Muller, I. Lukeš and J. A. Peters, *Bioconjugate Chem.*, 2004, 15.
11 C.-H. Huang, K. Nwe, A. A. Zaki, M. W. Brechbiel and A. Tsourkas, *ACS Nano*, 2012, **6**, 9416–9424.
12 Y. Li, M. Beija, S. Laurent, L. Vander Elst, R. N. Muller, H. T. T. Duong, A. B. Lowe, T. P. Davis and C. Boyer, *Macromolecules*, 2012, **45**, 4196–4204.
13 K. Luo, G. Lui, W. She, Q. Wang, G. Wang, B. He, H. Ai, Q. Gong, B. Song and Z. Gu, *Biomaterials*, 2011, 32.
14 M. Zhen, J. Zheng, L. Ye, S. Li, C. Jin, K. Li, D. Qiu, H. Han, C. Shu, Y. Yang and C. Wang, *ACS Appl. Mater. Interfaces*, 2012, **4**, 3724–3729.
15 T. N. Parac-Vogt, K. Kimpe, S. Laurent, L. Vander Elst, C. Burtea, F. Chen, R. N. Muller, Y. C. Ni, A. Verbruggen and K. Binnemans, *Chem. – Eur. J.*, 2005, **11**, 3077–3086.
16 P. Caravan, *Acc. Chem. Res.*, 2009, **42**, 851–862.
17 C. Henoumout, V. Henrotte, S. Laurent, L. Vander Elst, R. N. Muller and K. Binnemans, *J. Inorg. Biochem.*, 2008, **102**, 721–730.
18 F. Kielar, L. Tei, E. Terreno and M. Botta, *J. Am. Chem. Soc.*, 2010, **132**, 7836–7837.
19 T. N. Parac-Vogt, K. Kimpe, S. Laurent, C. Piérart, L. Vander Elst, R. N. Muller and K. Binnemans, *Eur. J. Inorg. Chem.*, 2004, 3538–3543.
20 C. Vanasschen, N. Bouslimani, D. Thonon and J. F. Desreux, *Inorg. Chem.*, 2011, **50**, 8946–8958.

21 E. Debroye and T. N. Parac-Vogt, *Chem. Soc. Rev.*, 2014, **43**, 8178–8192.
22 A. Louie, *Chem. Rev.*, 2010, **110**, 3146–3195.
23 L. Frullano and T. J. Meade, *J. Biol. Inorg. Chem.*, 2007, **12**, 939–949.
24 D. Jańczewski, Y. Zhang, G. K. Das, D. K. Yi, P. Padmanabhan, K. K. Bhakoo, T. T. Y. Tan and S. T. Selvan, *Microsc. Res. Technol.*, 2011, **74**, 568–576.
25 C. Bernhard, C. Goze, Y. Rousselin and F. Denat, *Chem. Commun.*, 2010, **46**, 8267–8269.
26 A. Keliris, T. Ziegler, R. Mishra, R. Pohmann, M. G. Sauer, K. Ugurbil and J. Engelmann, *Bioorg. Med. Chem.*, 2011, **19**, 2529–2540.
27 T. Koullourou, L. S. Natrajan, H. Bhavar, S. J. A. Pope, J. H. Feng, J. Narvainen, R. Shaw, E. Scales, R. Kauppinen, A. M. Kenwright and S. Faulkner, *J. Am. Chem. Soc.*, 2008, **130**, 2178–2179.
28 G. Dehaen, S. V. Eliseeva, K. Kimpe, S. Laurent, L. Vander Elst, R. N. Muller, W. Dehaen, K. Binnemans and T. N. Parac-Vogt, *Chem. – Eur. J.*, 2012, **18**, 293–302.
29 G. Dehaen, S. V. Eliseeva, P. Verwilst, S. Laurent, L. Vander Elst, R. N. Muller, W. Deborggraeve, K. Binnemans and T. N. Parac-Vogt, *Inorg. Chem.*, 2012, **51**, 8775–8783.
30 E. Debroye, G. Dehaen, S. V. Eliseeva, S. Laurent, L. Vander Elst, R. N. Muller, K. Binnemans and T. N. Parac-Vogt, *Dalton Trans.*, 2012, **41**, 10549–10556.
31 C. Gløgård, R. Hovland, S. L. Fossheim, A. J. Aasena and J. Klavenessa, *J. Chem. Soc., Perkin Trans. 2*, 2000, 1047–1052.
32 N. Kamaly, T. Kalber, G. Kenney, J. Bell, M. Jorgensen and A. Miller, *Org. Biomol. Chem.*, 2010, 8.
33 S. J. Soenen, G. V. Velde, A. Ketkar-Atre, U. Himmelreich and M. D. Cuyper, *Wiley Interdiscip. Rev.: Nanomed. Nanobiotechnol.*, 2011, **3**, 197–211.
34 W. J. Rieter, J. S. Kim, K. M. L. Taylor, H. An, W. Lin, T. Tarrant and W. Lin, *Angew. Chem., Int. Ed.*, 2007, **46**, 3680–3682.
35 P. Howes, M. Green, A. Bowers, D. Parker, G. Varma, M. Kallumadil, M. Hughes, A. Warley, A. Brain and R. Botnar, *J. Am. Chem. Soc.*, 2010, **132**, 9833–9842.
36 S. Ronchi, M. Colombo, P. Verderio, S. Mazzucchelli, F. Corsi, C. D. Palma, R. Allevi, E. Clementi and D. Prosperi, *AIP Conf. Proc.*, 2010, **1275**, 102–105.
37 D. Bhattacharya, M. Das, D. Mishra, I. Banerjee, S. K. Sahu, T. K. Maiti and P. Pramanik, *Nanoscale*, 2011, **3**, 1653–1662.
38 Y. Chen, H. Chen, S. Zhang, F. Chen, L. Zhang, J. Zhang, M. Zhu, H. Wu, L. Guo, J. Feng and J. Shi, *Adv. Funct. Mater.*, 2011, **21**, 270–278.
39 L. Vander Elst, A. Roch, P. Gillis, S. Laurent, F. Botteman, J. W. M. Bulte and R. N. Muller, *Magn. Reson. Med.*, 2002, **47**, 1121–1130.
40 G. K. Das, N. J. J. Johnson, J. Cramen, B. Blasiak, P. Latta, B. Tomanek and F. C. J. M. v. Veggel, *J. Phys. Chem. Lett.*, 2012, **3**, 524–529.
41 M. Norek, E. Kampert, U. Zeitler and J. A. Peters, *J. Am. Chem. Soc.*, 2008, **130**, 5335–5340.
42 P. Caravan, M. T. Greenfield and J. W. M. Bulte, *Magn. Reson. Med.*, 2001, **46**, 917–922.
43 A. Zhang, J. Zhang, Q. Pan, S. Wang, H. Jia and B. Xu, *J. Lumin.*, 2012, **132**, 965–971.
44 Y. Bi, X.-T. Wang, W. Liao, X. Wang, R. Deng, H. Zhang and S. Gao, *Inorg. Chem.*, 2009, 48.
45 M. Harris, S. Carron, L. Vander Elst and T. N. Parac-Vogt, *Eur. J. Inorg. Chem.*, 2015, 4572–4578.
46 E. Debroye, S. Laurent, L. Vander Elst, R. N. Muller and T. N. Parac-Vogt, *Chem. – Eur. J.*, 2013, **19**, 16019–16028.
47 M. Harris, S. Carron, L. Vander Elst, S. Laurent, R. N. Muller and T. N. Parac-Vogt, *Chem. Commun.*, 2015, **51**, 2984–2986.
48 C. Li and W. Wong, *J. Org. Chem.*, 2003, **68**, 2956–2959.
49 T. Hirayama, M. Taki, A. Kodan, H. Kato and Y. Yamamoto, *Chem. Commun.*, 2009, 3196–3198.
50 S. Laurent, T. N. Parac-Vogt, K. Kimpe, C. Thirifays, K. Binnemans, R. N. Muller and L. Vander Elst, *Eur. J. Inorg. Chem.*, 2007, 2061–2067.
51 H. Onishi and K. Sekine, *Talanta*, 1972, **19**, 473–478.
52 K. Driesen, R. V. Deun, C. Görller-Walrand and K. Binnemans, *Chem. Mater.*, 2004, **16**, 1531–1535.
53 T. Kimura and Y. Kato, *J. Alloys Compd.*, 1998, **275**, 806–810.
54 W. D. Horrocks and D. R. Sudnick, *J. Am. Chem. Soc.*, 1979, **101**, 334–340.
55 I. Hemmilä, S. Dakubu, V.-M. Mukkala, H. Siitari and T. Lövgren, *Anal. Biochem.*, 1984, **137**, 335–343.
56 I. Hemmilá and V.-M. Mukkala, *Crit. Rev. Clin. Lab. Sci.*, 2001, **38**, 441–519.
57 J. A. Keelan and J. T. France, *Clin. Chem.*, 1987, **33**, 2292–2295.
58 I. Hemmilä and V. Laitala, *J. Fluoresc.*, 2005, **15**, 529–542.
59 J. Feng, H.-J. Zhang, S.-Y. Song, Z.-F. Li, L.-N. Sun, Y. Xing and X.-M. Guo, *J. Lumin.*, 2008, **128**, 1957–1964.
60 S. Quici, M. Cavazzini, G. Marzanni, G. Accorsi, N. Armaroli, B. Ventura and F. Barigelletti, *Inorg. Chem.*, 2005, **44**, 529–537.
61 S. Viswanathan, Z. Kovacs, K. N. Green, S. J. Ratnakar and A. D. Sherry, *Chem. Rev.*, 2010, **110**, 2960–3018.
62 J. A. Peters, J. Huskens and D. J. Raber, *Prog. Nucl. Magn. Reson. Spectrosc.*, 1996, **28**, 283–350.
63 S. Torres, J. A. Martins, J. P. André, C. F. G. C. Geraldes, A. E. Merbach and É. Tóth, *Chem. – Eur. J.*, 2006, **12**, 940–948.
64 A. Accardo, D. Tesauro, L. Aloj, C. Pedone and G. Morelli, *Coord. Chem. Rev.*, 2009, **253**, 2193–2213.